RSC Advances

PAPER

View Article Online
View Journal | View Issue

Cite this: *RSC Adv.*, 2023, **13**, 7664

Synthesis of a new magnetic metal organic framework based on nickel for extraction of carvacrol and thymol in thymus and savory samples and analyzed with gas chromatography

Somaye Siahkamari [a] and Ali Daneshfar *[ab]

The present research aims at reporting a new sorbent, a magnetic nano scale metal–organic framework (MOF), based on nickel acetate and 6-phenyl-1,3,5-triazine-2,4-diamine. The prepared sorbent was used to extract carvacrol and thymol using an ultrasonic-assisted dispersive micro solid phase extraction (UA-DμSPE) method. The structure of the metal organic framework was studied by applying scanning electron microscopy (SEM), X-ray diffraction (XRD), Fourier transform infrared spectroscopy (FT-IR), energy dispersive spectrometry (EDS), and vibrating sample magnetometer (VSM). The effects of various parameters such as ionic strength of sample solution, amount of sorbent (mg), volume of eluent solvent (μL), vortex and ultrasonic times (min) were optimized. Under optimal conditions, the analytes resulted in determination coefficients (R^2) of 0.9985 and 0.9967 in the concentration range 0.01–2 μg mL^{-1}, and in limits of detection of 0.0025 and 0.0028 μg mL^{-1}. Significantly, this method can be successfully applied in order to determine the target analytes in spiked real samples. Notably, the relative mean recoveries range from 94.5 to 105.7%.

Received 19th November 2022
Accepted 22nd February 2023

DOI: 10.1039/d2ra07367f

rsc.li/rsc-advances

1. Introduction

Essential oils (EOs) are natural aromatic oily liquids, obtained from vegetal materials such as, leaves, twigs, bark, herbs, roots, wood and fruits.[1–3] Furthermore, EOs have antimicrobial, antioxidant, anti-carcinogenesis, antitussive and antibacterial activities.[4,5] Due to these properties, they are used in food, pharmaceutics and perfumes.[6–8] Moreover, the main phenolic components of EOs are carvacrol (5-isopropyl-2-methylphenol) and thymol (2-isopropyl-5-methylphenol). These isomeric monoterpene phenols – extracted from thyme, savory and oregano-are used in traditional medicine to treat cold, flu and cough and also as a cholagogue agent for bronchitis.[9–11] Due to the fact that carvacrol and thymol are widely used in pharmaceutical industries, various analytical procedures have been developed to extract and determine carvacrol and thymol in biological samples, including solid phase extraction (SPE), solid phase micro extraction (SPME) and head space extraction methods.[12–14]

It is worth mentioning that SPE, SPME and head space are time-consuming procedures, and are very expensive. In addition SPE require large amounts of toxic solvent and have a low sensitivity.[15–18] Thus, developing selective, sensitive, and specific methods to determine trace concentration of these samples are of great significance. Recently scientists tend to develop miniaturized sample preparation methods namely micro-extraction methods, among which. UA-DμSPE has been widely used as a pre-concentration method prior to chromatography analysis. UA-DμSPE is a miniaturized extraction method categorized as an SPE technique. Moreover, UA-DμSPE is based on two steps: adsorption and desorption. During the adsorption process, a small amount of solid sorbent (mg or ng range) is dispersed in an aqueous sample solution containing target analytes and using a magnetic stirrer, and an ultrasonic or a vortex device. In the desorption step, the adsorbed analytes are eluted *via* an appropriate solvent under sonicated conditions. Dispersion phenomenon enables the sorbent to rapidly and uniformly interact with all the target analytes – leading to enhance the precision of method and reduce the extraction time.[19–26]

Due to the importance of sorbent in extraction efficiency of DμSPE methods, developing new sorbents is very important to achieve high extraction efficiency and selectivity.[27] Metal–organic frameworks (MOFs) have been successfully used as sorbents for solid-phase microextraction, solid-phase extraction and sampling, and also as stationary phases for gas chromatography and liquid chromatography.[28]

MOFs are a new and emerging class of hybrid organic–inorganic crystalline solid materials characterized by their open

[a]*Department of Chemistry, Faculty of Science, Ilam University, P.O. Box 69315516, Ilam, Iran. E-mail: daneshfara@yahoo.com; adaneshfar@mail.ilam.ac.ir; daneshfar.a@Lur.ac.ir*

[b]*Department of Chemistry, Faculty of Science, Lorestan University, Khoramabad, Iran*

and porous structures.[29–31] MOFs are supramolecular assemblies which are composed of inorganic metal ions or metal ion clusters connected to organic linkers through strong coordination bonds-creating a material with an open, crystalline, porous and 3-D framework.[32–36]

Recently, MOFs have attracted great interest due to their unique characteristics such as high surface area, low density, chemical tenability, high thermal and mechanical stability, high flexibility, facile synthesis, and oriented crystal growth.[37–40] Accordingly, this material has been widely used in different fields; including, gas storage, gas purification and separation, energy storage, batteries, catalysis, heterogeneous (asymmetric) catalysis, ion-exchange, magnetism, imaging, drug delivery, luminescence, molecular sensing, guest molecule encapsulation, photovoltaics, and optics.[38,41–43]

Accordingly, the present work aims at developing a new, easy, low-cost and one-step synthesis of magnetic nanoscale metal–organic framework (MOF) based on nickel acetate and 6-phenyl-1,3,5-triazine-2,4-diamine (Ni-MOF).

In this paper, we created a novel metal–organic framework nanostructure. We believe this MOF has great potential for various applications in analytical chemistry. This compound is promising for extraction applications because of its good environmental stability, facile synthesis, and relatively low cost. Accordingly, by coupling with gas chromatography, the MOF was successfully applied to the extraction of carvacrol and thymol.

This operation is useful because of merging both benefits of MOF and D-μ-SPE method including (a) the fast and quantitative adsorption and desorption, (b) high surface area and capacity (c) high dispersibility in liquid samples and (d) easy to collect with an external magnet.

In order to characterize Ni-MOF, Fourier transform infrared spectroscopy (FT-IR), vibrating sample magnetometer (VSM), scanning electron microscopy (SEM), X-ray diffraction (XRD), and energy dispersive spectrometry (EDS) were used. In addition, Ni-MOF was used to extract carvacrol and thymol in thymus and savory samples-applying UA-DμSPE method. Furthermore, some key parameters for D-μSPE, *i.e.* vortex and ultrasonication time, extraction solvent (type and volume), amount of sorbent, ionic strength and pH, were optimized.

Finally, these compound used for extraction of thymol to explore the possibility of using these MOF as efficient adsorbent.

2. Experimental

2.1. Chemicals

Nickel acetate tetrahydrate (>99%), 6-phenyl-1,3,5-triazine-2,4-diamine (>98%), carvacrol (Car) (>98%), thymol (Thy) (>98%), phenol (internal standard, I.S.) (>99%), methanol (>98%), ethanol (>98%), acetonitrile (>99%), dichloromethane (>99.8%), chloroform (>99%), tetrahydrofuran (THF) (>99%), acetone (>99%), sodium chloride (>99%), hydrochloric acid (>35%), sodium hydroxide (>98%) and dimethylformamide (DMF) (>99%) were obtained from Merck (Darmstadt, Germany). All chemicals were used as purchased without any further purification. Doubly distilled water was also used in preparing all solutions.

2.2. Apparatus

Experiments were performed using a gas chromatograph (GC-17, Shimadzu, Japan) that included a flame ionization detector and a BP10 capillary column (25 m in length, 0.32 mm in internal diameter, and 0.25 millimeters in film thickness). As the carrier gas, helium with a purity level of 99.9999% was employed. The splitless mode was used for operation of the intake. The following temperature settings were programmed into the oven: starting temperature of 50 °C, which was maintained for 2 minutes, and ramped up to 240 °C at a rate of 10 °C per minute (held for 5 min). Both the injector and the detector were heated to temperatures of 280 and 300 °C, respectively. Moreover, X-ray diffraction (XRD) pattern was obtained on a diffractometer (Bruker D8/Advance X-ray, Germany). SEM images were recoded to visualize the morphology and size of magnetic NPs using Hitachi S4160 (Japan). A pH-meter (OHAUS, Model ST5000-USA) with a double junction glass electrode was used to measure the acidity of the solutions. The magnetic properties of Ni-MOF were determined using vibrating sample magnetometer (VSM, MDKFD-Iran). Finaly, regarding adsorption and desorption treatments, a 50/60 Hz, 35 W vortex mixer (Daihan Scientific, VM10, Korea) and an ultrasonic-bath equipped with digital timer and temperature controller (Bandelin Sonorex, RK103H, Germany) at 35 kHz of frequency and 140/560 of power were utilized, respectively.

2.3. Synthesis of Ni-MOF NPs

The metal organic framework based on nickel was synthesized from nickel acetate using a solvothermal method. Briefly, 0.744 g of nickel acetate and 0.561 g of 6-phenyl-1,3,5-triazine-2,4-diamine were dissolved in 20 mL of DMF and, then, the mixture was transferred into a stainless-steel autoclave (NANOSIZE, Iran) and heated at 150 °C for 48 h in an oven. Afterwards, the autoclave was cooled to room temperature (about 25 °C). The resulting particles were collected using an external magnet, washed several times with water and ethanol and, finally, dried in an oven at 50 °C.

2.4. UA-DμSPE based on Ni-MOF procedure

Primarily, 5 mL aqueous standard sample-containing 0.05 μg mL^{-1} of carvacrol and thymol was mixed with 2 mg nanosorbent (Ni-MOF) in test tube. Afterwards, the test tube was shaken for an appropriate time (2–40 min) on a vortex agitator (VM-10 DAIHAN, Korea) to equilibrate the adsorption process. Subsequently, the dispersed Ni-MOF nanosorbent was separated from the solution using an external magnet and, then, the supernatant was discarded. In the next step, regarding the back-extraction of carvacrol and thymol from sorbent, an adequate volume (25–225 μL) of desorption solvent (containing internal standard) was added to the test tube and, then, the Ni-MOF sorbent was re-dispersed under ultrasonication (DT31H, Bandelin Germany) at an appropriate time (1–30 min). Separation of particles from the organic phase was carried out using an

external magnet. Afterwards, the organic phase containing the eluted analytes was collected and, then 0.5 μL of it was manually injected into the GC-FID system for further analysis.

2.5. Preparation of standard solution and samples

Stock standard solutions of carvacrol and thymol (1000 mg L^{-1}) and I.S. (100 mg L^{-1}) were prepared in methanol. Working solutions were obtained *via* appropriate dilution of the stock standard solution with double distilled water. The solutions were stored in a suitable container and, then, kept at refrigerator (4 °C) in the dark place. Calibration standards were made at different concentration ranges, each one having three replicates. Furthermore, two plant materials (thymus, savory) were provided from Ilam Province, Iran. After identification, the samples were cleaned, air-dried and, finely, grounded. Subsequently, the extract was prepared *via* successive maceration of the powder. As follows, 5 mL of MeOH/water (80 : 20%) mixture was added to 0.2 g of samples. The mixture was sonicated for 20 min and, then, left in room temperature for 48 h. Afterwards, the mixture was centrifuged and filtered and, then, the supernatant was separated and stored at 4 °C for subsequent experiments.

3. Results and discussion

3.1. Characterization of Ni-MOFNPs

FT-IR, XRD, EDS, SEM and VSM analyses were applied in order to investigate the prepared MOF. Fig. 1 shows the FT-IR analysis of Ni-MOF. Regarding the FT-IR spectrum of Ni-MOF at 1375 and 1568 cm^{-1}, there are two intensive peaks that should be attributed to the asymmetric and symmetric stretching modes of the coordinated group (–COO–). The strong band at 3605 cm^{-1} is associated with the stretching vibrations of OH.[29]

The crystal structures of Ni-MOF nanoparticles are characterized applying XRD, as shown in Fig. 2. The XRD patterns of Ni-MOF revealed the diffraction peaks at 44.76, 52.11, and 76.56 corresponding to Miller indices, (1 1 1) (2 0 0) (2 2 0), which are in good agreement with the standard XRD cards (JCPDS No. 01-070-0989). The crystallite size was estimated from the width of (1 1 1) plane according to the Scherer's formula. It is obvious from the XRD patterns that the Ni-MOF crystals have cubic (fcc) structures.[33]

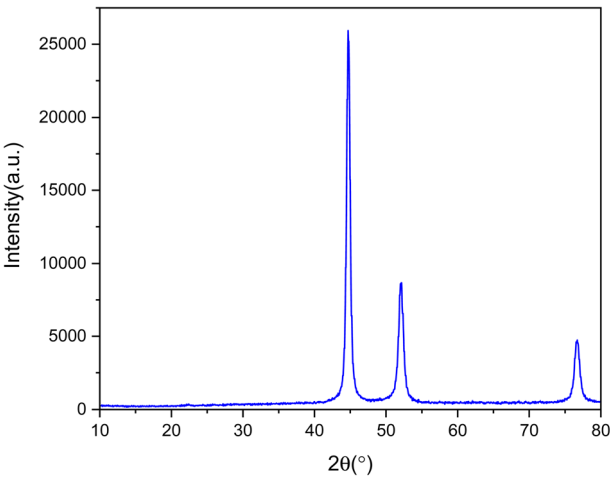

Fig. 2 XRD pattern of the Ni-MOF.

Moreover, the components of Ni-MOF were analyzed using EDS, as plotted in Fig. 3. The obtained data reveal that Ni, C, N, and O are dispersed throughout the particle.

The morphology and structure of the synthesized Ni-MOF were investigated using SEM images, as shown in Fig. 4. According to SEM images, it can be clearly observed that Ni-MOF formed a homogeneous base with spherical shape having regular sizes and average diameters of approximately 500 nm.

The vibration sample magnetometry curve of Ni-MOF is shown in Fig. 5. The saturation magnetization value for Ni-MOF was 71.77, emu g^{-1}. Significantly, the relatively high saturation magnetization value of Ni-MOF made this sorbent sensitive to magnetic fields and easy to isolate from aqueous solution.

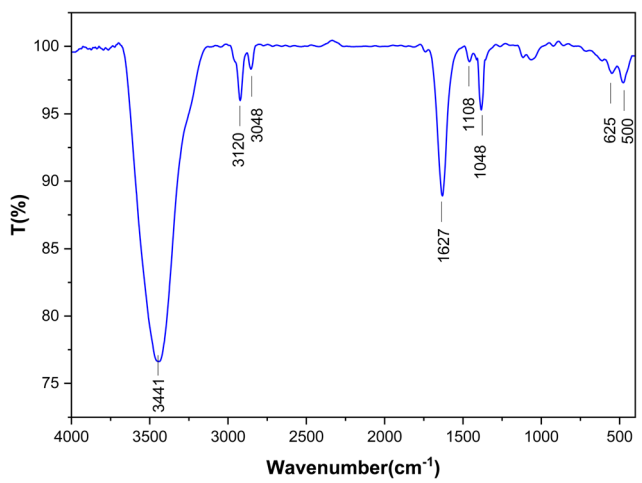

Fig. 1 FT-IR spectra of the Ni-MOF.

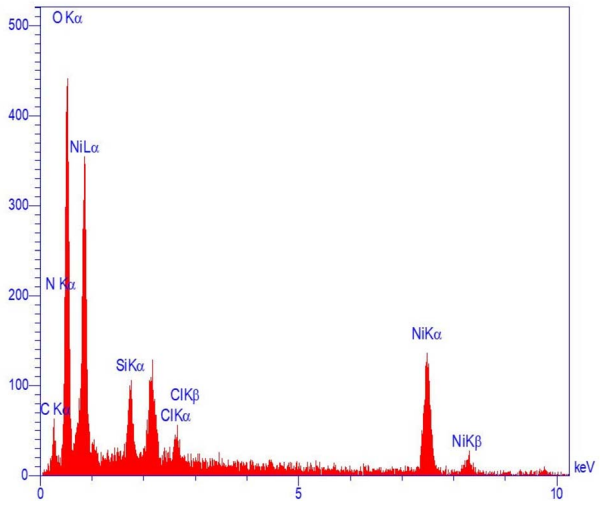

Fig. 3 EDS spectrum of the Ni-MOF.

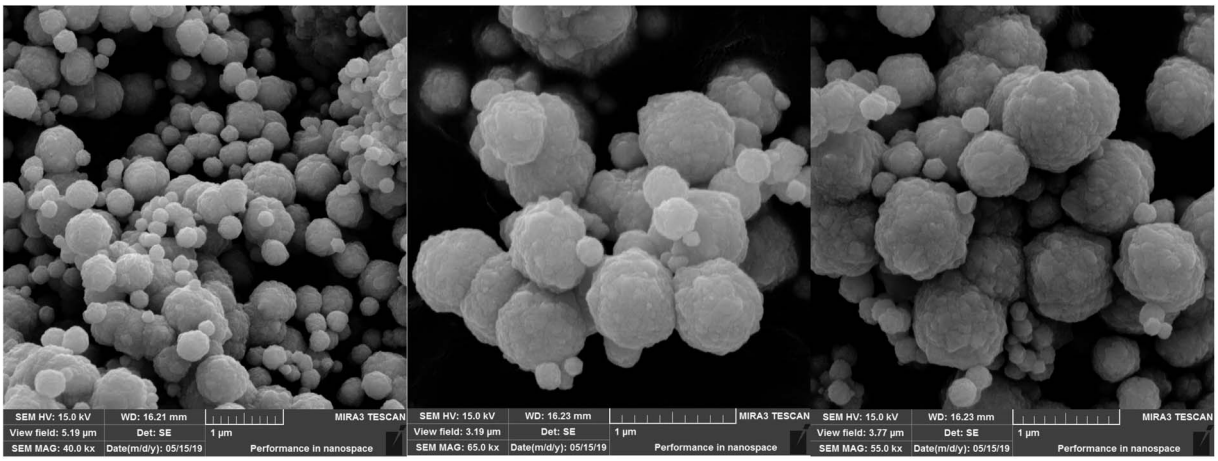

Fig. 4 SEM images of the Ni-MOF.

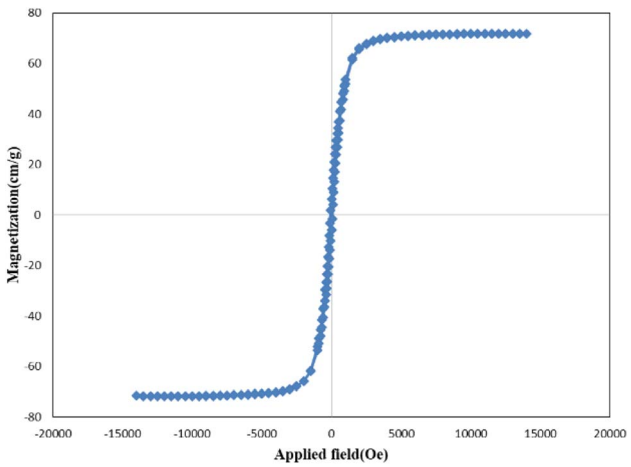

Fig. 5 Vibration sample magnetometry curve of the Ni-MOF.

Accordingly, the chemical composition and structure of the Ni-MOF system can be predicted based on 3d orbitals. Based on our knowledge, when a transition metal ion with 3d orbital such as Ni is used, Ni ion should be chelated by four ligands to give a neutral Ni-MOF unit. In this sense, the lone pair electrons of the uncoordinated nitrogens in ligands (6-phenyl-1,3,5-triazine-2,4-diamine) would be useful to interact with the 3d orbital of the Ni ions, whose 3d orbitals in Ni ions act as an electron-acceptor agent. The proposed structure is shown in Scheme 1.

3.2. Optimization of the analytical procedure

3.2.1. Effect of extraction solvent. The choice of extraction solvent is essential in UA-DμSPE to achieve efficient extraction of the analytes. The extraction solvent has to meet certain factors such as low volatility, extraction capability of target analytes, and good chromatographic behavior. Based on these considerations, several organic solvents-having various polarities including THF, methanol, ethanol, acetone, acetonitrile, chloroform and dichloromethane-were used as extraction solvent. The experiments were performed using 50 μL extraction solvent from 5 mL working solutions in pH 9, for 15 min vortex time. Fig. 6 depicts the enrichment factor as a function of extraction solvent. The results indicate that the best elution of

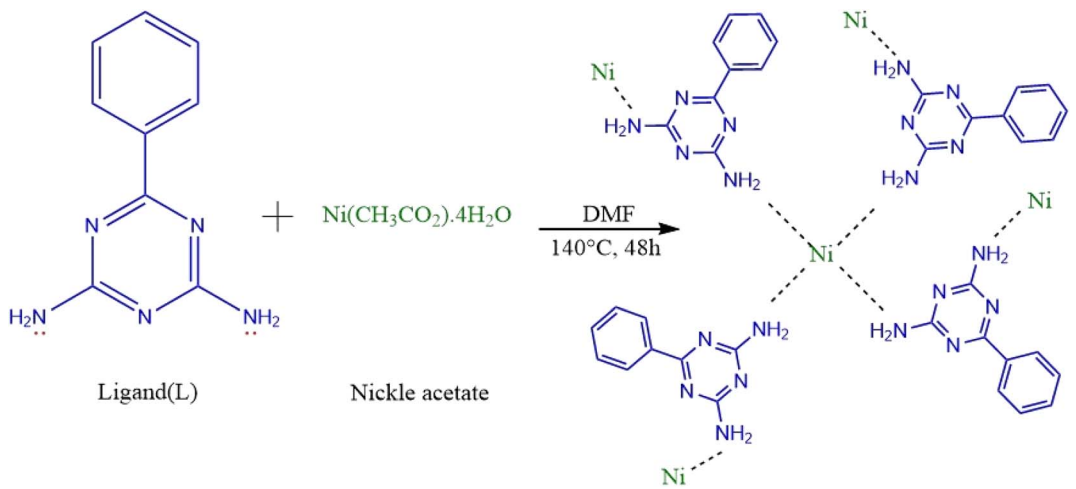

Scheme 1 Proposed structure for Ni-MOF.

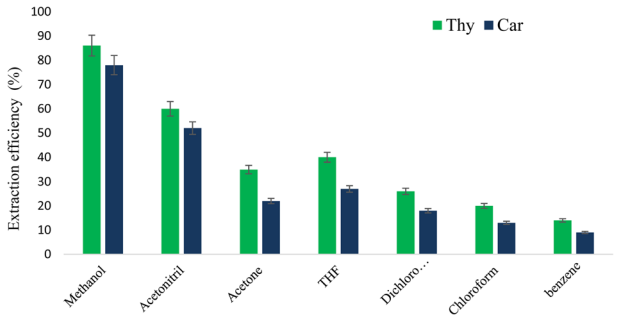

Fig. 6 Effect of extraction organic solvent on the extraction efficiency.

target analytes was performed using methanol, whereas dichloromethane had the lowest extraction efficiency for the two analytes. As it is illustrated when methanol is used, the extraction efficiency of carvacrol and thymol were more than 80%, which would be dramatically higher than extraction efficiency obtained by other solvents. Therefore, methanol was selected as the most appropriate extraction solvent for subsequent UA-DμSPE experiments. This can be explained by the fact that the similarity of polarity between target analytes and methanol is superior to other solvents.

3.2.2. Effect of pH of sample solution. The extraction efficiency and adsorption mechanism of the analyte depend on pH of the sample solution, which was investigated in a pH range of 2.0 to 11.0. Fig. 7A shows the extraction efficiencies as a function of pH. Values of pH higher than 11.0 were not examined, because carvacrol and thymol are weak acidic compounds that can be hydrolyzed at basic pH. The maximum desorption of carvacrol and thymol and their extraction were obtained at pH 9. The net charge of carvacrol and thymol molecule dramatically

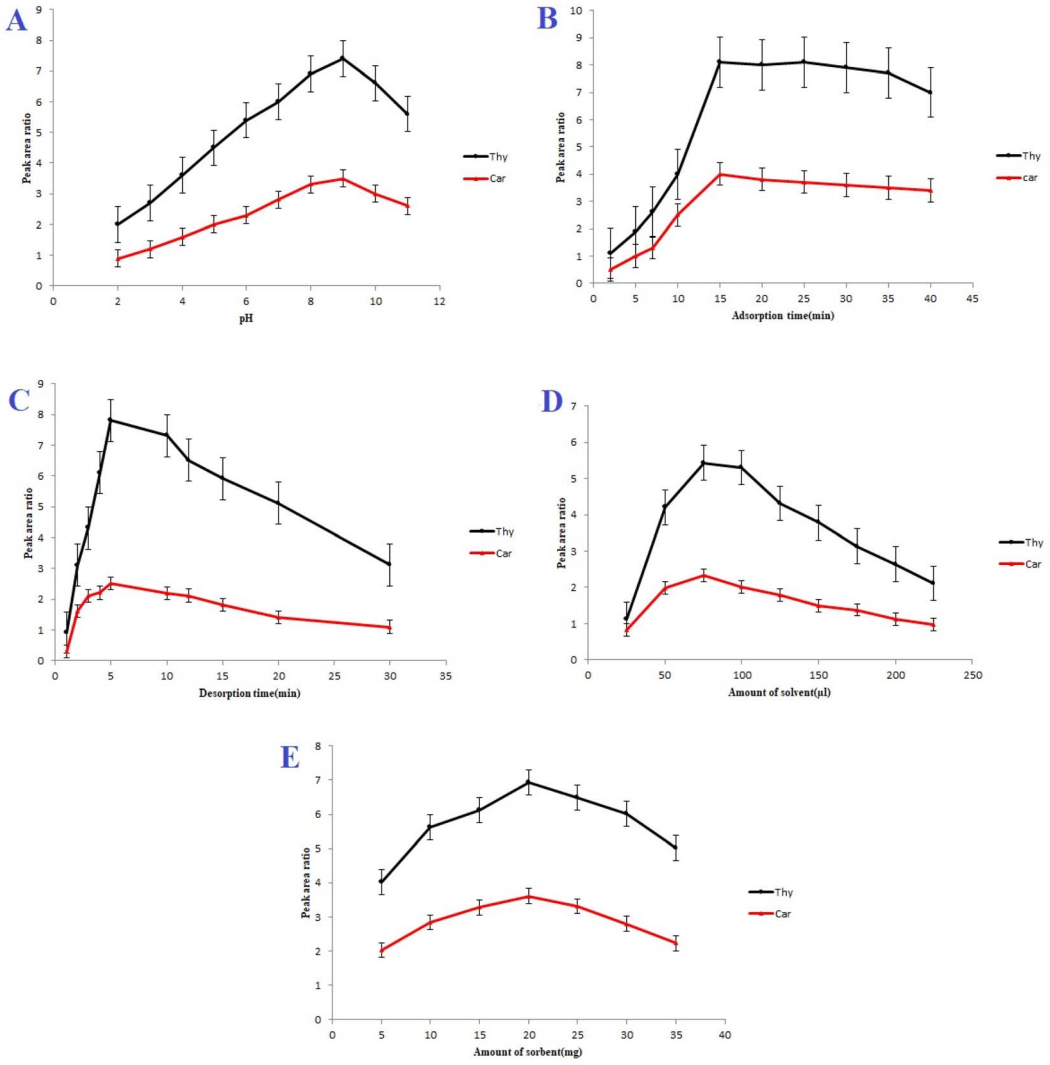

Fig. 7 (A) Effect of pH. Volume of extraction solvent = 50 μL; amount of sorbent = 20 mg; and ultrasonic time = 5 min; (B) effect of adsorption time. Volume of eluent = 50 μL; pH 9; amount of sorbent = 20 mg; and ultrasonic time = 5 min; (C) effect of desorption time. Volume of eluent = 50 μL; pH 9; amount of sorbent = 20 mg; and vortex time = 10 min; (D) effect of the volume of eluent solvent; pH 9; amount of sorbent = 20 mg; vortex time = 10 min; and ultrasonic time = 5 min; (E) effect of sorbent dosage. Volume of eluent solvent = 75 μL; pH 9; vortex time = 10 min; and ultrasonic time = 5 min.

changed with pH of the medium pH (Fig. 7A). Under acidic conditions, the amino groups on the surface of Ni-MOF may be protonated. Regarding the basic pH, carvacrol and thymol are hydrolyzed. Based on the above results, a pH of 9 was used for subsequent experiments.[47]

3.2.3. Effect of adsorption time (vortex time). The adsorption between targets and the Ni-MOF particles is an equilibrium-based process. Sufficient adsorption time, hence, is indispensable for adsorption equilibrium. Extraction was accelerated in the aid of vortex by thorough exposure to each other within the mixture system. The effect of adsorption time on the extraction efficiencies of Car and Thy was examined from 2 min to 40 min. As demonstrated in Fig. 7B, the extraction efficiencies increased while increasing adsorption time and, significantly, the highest peak area ratios were reached at a 15 min. After 15 min, no increase in the extraction efficiency was observed while time and the extraction efficiency was approximately constant. Therefore, all further experiments were performed with adsorption time of 15 min.

3.2.4. Effect of desorption time (ultrasonic time). Ultrasound time is the most important parameter affecting the extraction of analyst in UA-DμSPE method. Fig. 7C clearly demonstrates the effect of ultrasound time on the extraction of carvacrol and thymol in the range of 1–30 min. The results show that while increasing the desorption time up to 5 min, the peak area ratio also increased. After 5 min, the extraction efficiency decreased. This decrease in extraction efficiency may be explained as follows: (a) the possible degradation of Ni MOF, (b) evaporation of methanol, and (c) when the ultrasonic time increases, the temperature of the sample solution rises, leading to a new equilibrium of analytes between the sorbent and the extraction solvent.[48] Therefore, all further experiments were performed with desorption time of 5 min.

3.2.5. The effect of the volume of extraction solvent. The impact of extraction solvent volume on carvacrol and thymol recovery was studied and optimized in the range of 25–225 μL. As it can be seen 5 in Fig. 7D, the maximum extraction efficiency was obtained when the volume of extraction solvent was 75 μL.

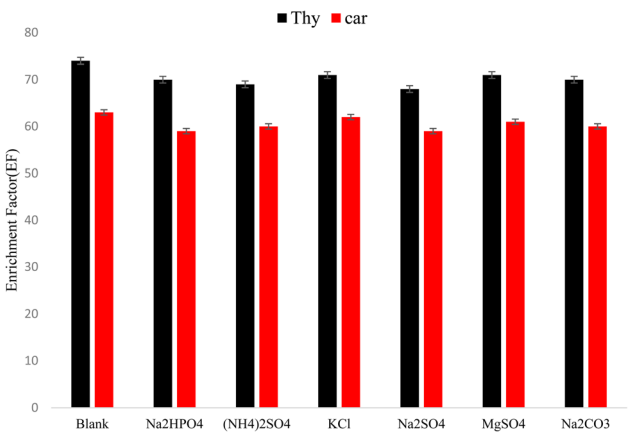

Fig. 8 Effect of ion matrix. Extraction conditions: amount of sorbent = 20 mg; pH 9; volume of eluent solvent = 75 μL; adsorption time = 15 min; desorption time = 5 min.

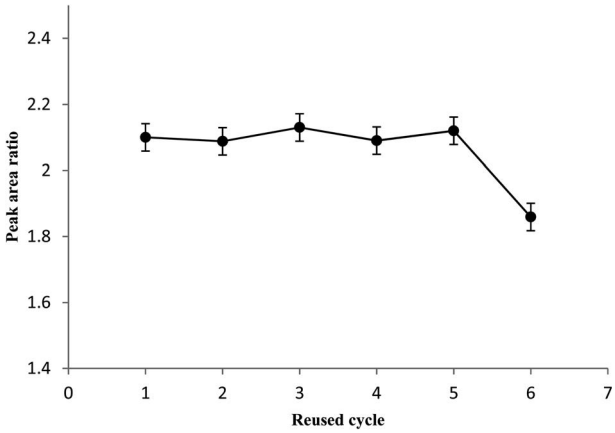

Fig. 9 Reusability of Ni-MOF on the average peak area.

The results show that the extraction efficiency decreases with increasing volume extraction solvent more than 75 μL. This decreases may be attributed to more dilution effect. Moreover, regarding volumes less than 75 μL, the solvent was not able to extract the analytes. Therefore, 75 μL was selected as the optimum volume for this parameter.

3.2.6. The effect of amount of sorbent. The effect of the amount of sorbent on the extraction efficiency was studied in the range from 5.0 to 35.0 mg. The results illustrated in Fig. 7E indicate that, while increasing the sorbent amount from 5 mg to 20 mg extraction efficiency raises. Regarding amounts lower than 20 mg, the available surface area of sorbent is inadequate for a quantitative recovery of analytes. Furthermore, considering amounts more than 20 mg, the sorbent cannot be easily dispersed in aqueous sample and, consequently, the extraction efficiency of target analytes decreases. Thus, the 20 mg amount of sorbent was chosen for further experiments.

3.2.7. Effect of ion matrix. Effect of different cations and anions on the proposed method was investigated (Fig. 8). Different ions (10% w/w) in optimal condition were added to 2 mL of working solutions. As shown, due to chemical structures of carvacrol and thymol, none of these ions has

Table 1 Results from recovery of carvacrol and thymol in thymus and savory samples (n = 3)

Sample	Compounds	Amount add (μg mL^{-1})	RSD	Recovery (%)
Thymus	Thymol	10	3.6	94.5
		25	3.5	98.3
		50	3.9	101.6
	Carvacrol	10	4.3	103.3
		25	4.0	95.1
		50	4.2	104.2
Savory	Thymol	10	3.8	96.2
		25	3.4	97.2
		50	4.2	94.9
	Carvacrol	10	3.0	105.7
		25	3.9	96.8
		50	4.1	98.8

a significant effect on the extraction efficiencies of carvacrol and thymol.[44]

3.2.8. Recovery and reusability of the Ni-MOF. Regarding the reusability test after extraction procedure, the magnetic metal organic framework was separated using a magnet, washed with acetonitrile and deionized water and, then, dried in an oven. The same experiment was repeated to test the reusability of sorbent. The results of reusability test (Fig. 9) showed that carvacrol and thymol extraction in the first five cycles did not significantly decrease. After the fifth cycle, the extraction of analytes reduced by up to 11%.

3.3. Method validation

Under the optimum conditions, limits of detection (LOD), linear dynamic ranges (LDR), and enrichment factors (EFs) of the proposed method were calculated. The calibration graph

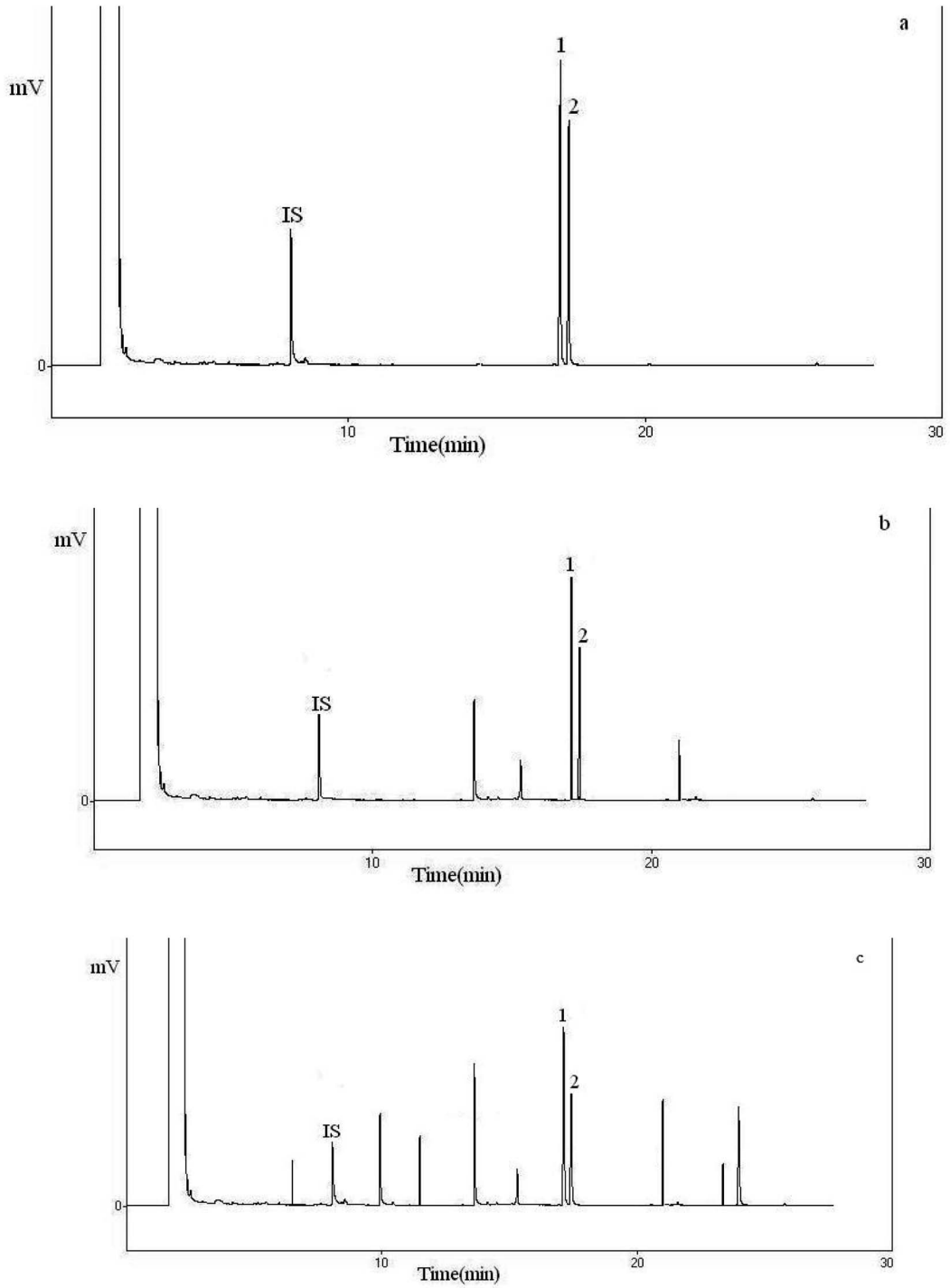

Fig. 10 GC-FID chromatograms obtained from different samples. (a) Standard (100.0 mg L^{-1}), (b) thymus; (c) savory. Peak identification: 1, thymol; 2, carvacrol; I.S., internal standard. Based on optimum extraction conditions.

Table 2 Comparsion of present method with reported methods for the determination of thymol and/or carvacrol

Method	Linear range (μg mL^{-1})	r^2	LOD	RSD%	Time (min)	Solvent	Volume of solvent (μL)	Ref.
HD-HSME[a]	1.25–87.5	0.9944–0.9979	0.23–1.87	6.37–11.8	5	*n*-Pentadecane	3	45
HPLC-ECD[b]	0.01–16		NR[f]	1.1–3.4		—	—	46
DI-SPME[c]	1–80	NR	0.6–0.8	6.8–12.7	60	Acetonitrile	100	47
UAME-NMSPD[d]	0.005–2	0.9993	0.00021–0.00023	3.12–3.25	10	Acetonitrile	600	48
HS-SPME[e]	0.002–4	0.9994–0.9997	0.00057–0.00089	NR	45	NR	—	49
UA-DμSPE	0.01–2	0.996	0.0025–0.0028	4.3	15	Methanol	75	This work

[a] Hydrodistillation-headspace solvent microextraction. [b] Liquid chromatography-electrochemical detection. [c] Direct-immersion solid-phase microextraction. [d] Ultrasound assisted microextraction-nano material solid phase dispersion. [e] Headspace-solid-phase microextraction. [f] Not reported.

was constructed *via* plotting the chromatographic peak area ratio of the analytes against the corresponding concentrations with 10 levels in the range of 0.005–5 μg mL^{-1}. The linear dynamic ranges (LDRs) were 0.01–2 μg mL^{-1} with good determination coefficients (R^2) of 0.9985, and 0.9967, for carvacrol and thymol, respectively. LOD values were equal to 0.0025 and 0.0028 μg mL^{-1} for thymol and carvacrol, respectively. The enrichment factors (EFs) were in the range of 153–168.

3.4. Real sample analysis

Thymus and savory samples were analyzed to validate the accuracy and applicability of the above mention proposed method. The recovery (%) and relative standard deviation (RSD) were summarized in Table 1. According to the results, the recoveries of carvacrol and thymol from thymus and savory samples, ranging from 94.5 to 105.7% with RSDs less than 4.3%. Representative chromatograms of the standard solution are shown in Fig. 10. As it can be observed, the peaks of analytes are free of interference peaks.

3.5. Comparison of this method with other methods

The proposed UA-DμSPE method (this method) coupled with GC-FID was compared to some reported methods based on some characteristics such as: linear dynamic range, LOD, RSD, recovery, extraction time, and type and volume of extraction solvent for the extraction and the determination of carvacrol and/or thymol in different matrices. The results are summarized in Table 2. As it can be seen, the characteristics parameters UA-DμSPE is comparable with other reported methods.

The proposed UA-DμSPE method (this method) coupled with GC-FID was compared to some reported methods for the extraction and the determination of carvacrol and/or thymol in different matrices. The results are summarized in Table 2. The proposed UA-DμSPE method (this method) coupled with GC-FID was compared to some reported methods based on some characteristics such as: linear dynamic range, LOD, RSD, recovery, extraction time, and extraction solvent for the extraction and the determination of carvacrol and/or thymol in different matrices. The results are summarized in Table 2. As it can be seen, the characteristics parameters UA-DμSPE is comparable with other reported methods.

4. Conclusions

Ultrasonic-assisted dispersive micro solid phase extraction (UA-DμSPE) method followed by GC-FID was developed to determine carvacrol and thymol. The proposed method is simple, sensitive, accurate, and inexpensive. The nanosized Ni-MOF with a large surface area and porosity can adsorb some organic compounds such as essential oils; therefore, Ni-MOF can be applied in extraction of carvacrol and thymol. The magnetic metal organic framework also shows satisfactory reusability in the five-cycle tests. The Ni-MOF showed favorable extraction efficiency due to hydrogen bonding interactions of the sorbent with the carvacrol and thymol. The results from validation indicate the proposed method can be applied to determine carvacrol and thymol in thymus and savory samples.

Conflicts of interest

There are no conflicts to declare.

Acknowledgements

This work was supported by the research facilities of Ilam University, Ilam, Iran.

References

1 S. Smaoui, H. Ben Hlima, L. Tavares, K. Ennouri, O. Ben Braiek, L. Mellouli, S. Abdelkafi and A. Mousavi Khaneghah, *Food Control*, 2022, **132**, 108566.
2 A. R. Mukurumbira, R. A. Shellie, R. Keast, E. A. Palombo and S. R. Jadhav, *Food Control*, 2022, **136**, 108883.
3 A. G. Evangelista, J. A. F. Corrêa, A. C. S. M. Pinto and F. B. Luciano, *Crit. Rev. Food Sci. Nutr.*, 2022, **62**, 5267.
4 N. J. Sadgrove, G. F. Padilla-González and M. Phumthum, *Plants*, 2022, **11**, 789.
5 C. Rossi, C. Chaves-López, A. Serio, M. Casaccia, F. Maggio and A. Paparella, *Crit. Rev. Food Sci. Nutr.*, 2022, **62**, 2172.
6 M. A. O. Dawood, M. F. El Basuini, S. Yilmaz, H. M. R. Abdel-Latif, M. Alagawany, Z. A. Kari, M. K. A. Abdul Razab, N. K. A. Hamid, T. Moonmanee and H. Van Doan, *Animals*, 2022, **12**, 823.

7 W. Zhang, H. Jiang, J.-W. Rhim, J. Cao and W. Jiang, *Food Chem.*, 2022, **367**, 130671.
8 A. Nair, R. Mallya, V. Suvarna, T. A. Khan, M. Momin and A. Omri, *Antibiotics*, 2022, **11**, 108.
9 G. V S, S. Johari, P. C and D. R, *ECS Trans.*, 2022, **107**(1), 17651.
10 A. M. B. Costa, A. R. S. T. Silva, A. de J. Santos, J. G. Galvão, V. V. Andrade-Neto, E. C. Torres-Santos, M. M. Ueki, L. E. Almeida, V. H. V. Sarmento, S. S. Dolabella, R. Scher, A. A. M. Lira and R. de S. Nunes, *Acta Trop.*, 2023, **237**, 106744.
11 R. Damiescu, D. Y. W. Lee and T. Efferth, *Pharmaceuticals*, 2022, **15**, 1387.
12 N. B. Rathod, P. Kulawik, F. Ozogul, J. M. Regenstein and Y. Ozogul, *Trends Food Sci. Technol.*, 2021, **116**, 733.
13 L. A. Sampaio, L. T. S. Pina, M. R. Serafini, D. dos S. Tavares and A. G. Guimarães, *Front. Pharmacol.*, 2021, 12702487.
14 C. M. Natal, M. J. G. Fernandes, N. F. S. Pinto, R. B. Pereira, T. F. Vieira, A. R. O. Rodrigues, D. M. Pereira, S. F. Sousa, A. G. Fortes, E. M. S. Castanheira and M. S. T. Gonçalves, *RSC Adv.*, 2021, **11**, 34024.
15 J. da Silva Sousa, H. O. do Nascimento, H. de Oliveira Gomes and R. F. do Nascimento, *Microchem. J.*, 2021, **168**, 106359.
16 M. Feng, C. Li, C. Wang, G. Zhu, J. Lu, Y. Chen, D. Xiao and X. Guo, *Int. J. Food Prop.*, 2022, **25**, 2445.
17 D. Armada, M. Celeiro, T. Dagnac and M. Llompart, *J. Chromatogr. A*, 2022, **1668**, 462911.
18 M. S. Kader and M. R. T. Rahman, in *Techniques to Measure Food Safety and Quality*, Springer International Publishing, Cham, 2021, p. 219.
19 P. Mohammadi, M. Ghorbani, P. Mohammadi, M. Keshavarzi, A. Rastegar, M. Aghamohammadhassan and A. Saghafi, *Microchem. J.*, 2021, **160**, 105680.
20 S. Zarabi, R. Heydari and S. Z. Mohammadi, *Microchem. J.*, 2021, **170**, 106676.
21 H. Sahebi, S. Massoud Bahrololoomi Fard, F. Rahimi, B. Jannat and N. Sadeghi, *Food Chem.*, 2022, **396**, 133637.
22 D. Wang, X. Chen, J. Feng and M. Sun, *J. Chromatogr. A*, 2022, **1675**, 463157.
23 P. Khodayari, N. Jalilian, H. Ebrahimzadeh and S. Amini, *J. Chromatogr. A*, 2021, **1655**, 462484.
24 D. C. de Andrade, S. A. Monteiro and J. Merib, *Adv. Sample Prep.*, 2022, **1**, 100007.
25 J. M. Jimenez-Soto, S. Cardenas and M. Valcarcel, *Anal. Chim. Acta*, 2012, **714**, 76.
26 A. R. Fontana, N. B. Lana, L. D. Martinez and J. C. Altamirano, *Talanta*, 2010, **82**, 359.
27 X. Jiang, M. Wu, W. Wu, J. Cheng, H. Zhou and M. Cheng, *Anal. Methods*, 2014, **6**, 9712.
28 S. Pezhhanfar, M. A. Farajzadeh, S. A. Hosseini-Yazdi and M. R. A. Mogaddam, *J. Food Compos. Anal.*, 2021, **104**, 104174.
29 M. Koolivand, M. Nikoorazm, A. Ghorbani Choghamarani and M. Mohammadi, *Appl. Organomet. Chem.*, 2022, **36**, e6656.
30 Z. Zhuang and D. Liu, *Nano-Micro Lett.*, 2020, **12**, 132.
31 T. Gorai, W. Schmitt and T. Gunnlaugsson, *Dalton Trans.*, 2021, **50**, 770.
32 S. M. Ramish, A. Ghorbani-Choghamarani and M. Mohammadi, *Sci. Rep.*, 2022, **12**, 1479.
33 A. Ghorbani-Choghamarani, Z. Taherinia and M. Mohammadi, *Environ. Technol. Innovation*, 2021, **24**, 102050.
34 B. Li, Y. F. Wang, L. Zhang and H. Y. Xu, *Chemosphere*, 2021, 132954.
35 J. Wales, D. Hughes, E. Marshall and P. Chambers, *Ind. Eng. Chem. Res.*, 2022, **61**, 9529.
36 B. Ogunbadejo and S. Al-Zuhair, *Molecules*, 2021, **26**, 680.
37 F. Ghobakhloo, D. Azarifar, M. Mohammadi, H. Keypour and H. Zeynali, *Inorg. Chem.*, 2022, **61**, 4825.
38 J. Fonseca, T. Gong, L. Jiao and H.-L. Jiang, *J. Mater. Chem. A*, 2021, **9**, 10562.
39 H. Zhang, X. Hu, T. Li, Y. Zhang, H. Xu, Y. Sun, X. Gu, C. Gu, J. Luo and B. Gao, *J. Hazard. Mater.*, 2022, **429**, 128271.
40 B. Mohan, S. Kumar, H. Xi, S. Ma, Z. Tao, T. Xing, H. You, Y. Zhang and P. Ren, *Biosens. Bioelectron.*, 2022, **97**, 113738.
41 N. Hussain-Khil, A. Ghorbani-Choghamarani and M. Mohammadi, *Sci. Rep.*, 2021, **11**, 15657.
42 D. Yang, Y. Chen, Z. Su, X. Zhang, W. Zhang and K. Srinivas, *Coord. Chem. Rev.*, 2021, **428**, 213619.
43 Y. Lin, Y. Li, Y. Cao and X. Wang, *Chem.–Asian J.*, 2021, **16**, 3281–3298.
44 Sh. babaee and A. daneshfar, *Anal. Methods*, 2016, **8**, 1489.
45 V. Kiyanpour, A. R. Fakhari, R. Alizadeh, B. Asghari and M. Jalali-Heravi, *Talanta*, 2009, **79**, 695–699.
46 G. Hui, W. Cao, L. Yan, C. Ni, B.-n. Wang and J.-b. Zheng, *Chromatographia*, 2010, **72**, 361–363.
47 A. Ghiasvand, S. Dowlatshah, N. Nouraei, N. Heidari and F. Yazdankhah, *J. Chromatogr. A*, 2015, **1406**, 87–93.
48 M. Roostaa, M. Ghaedi, A. Daneshfar and R. Sahrae, *J. Chromatogr. B: Anal. Technol. Biomed. Life Sci.*, 2015, **975**, 34–39.
49 G. M. L. Fiori, P. S. Bonato, M. P. M. Pereira, S. H. T. Contini and A. M. S. Pereira, *J. Braz. Chem. Soc.*, 2013, **24**, 837–846.